

Received 25 October 2023; revised 30 November 2023; accepted 30 November 2023. Date of publication 7 December 2023; date of current version 30 January 2024.

Digital Object Identifier 10.1109/OJAP.2023.3340336

# High-Permittivity Dielectric Half-Loop Yagi-Uda Antenna With End-Fire Radiation

WEN ZHENG<sup>1</sup>, SHIYAN WANG<sup>1</sup> (Member, IEEE), MENGJIAO TANG<sup>1</sup>,  
GANG ZHANG<sup>1</sup> (Senior Member, IEEE), WANG REN<sup>2</sup>, AND CHANGZHOU HUA<sup>3</sup> (Member, IEEE)

<sup>1</sup>Jiangsu Key Laboratory of 3D Printing Equipment and Manufacturing, Nanjing Normal University, Nanjing 210023, China

<sup>2</sup>School of Information and Electronic Engineering, Zhejiang Gongshang University, Hangzhou 310018, China

<sup>3</sup>Faculty of Electrical Engineering and Computer Science, Ningbo University, Ningbo 315211, China

CORRESPONDING AUTHORS: S. WANG and C. HUA (e-mail: nustwang@163.com; huachangzhou@126.com)

This work was supported in part by the National Natural Science Foundation of China under Grant 62101271 and Grant 62271273; in part by the Natural Science Foundation of Jiangsu Province for Youth under Grant BK20210557; in part by the Natural Science Foundation of Ningbo under Grant 2022J097; and in part by the Basic Public Welfare Research Plan and Natural Science Foundation of Zhejiang Province under Grant LGG19F010005.

**ABSTRACT** In this paper, a kind of half-loop Yagi-Uda antenna made of high-permittivity dielectric is proposed to realize end-fire radiation. As two typical materials with high permittivity, low-loss zirconia ceramic and liquid pure water are here employed for the proposed antenna to attain high radiation efficiency and support the characteristic of pattern reconfigurability, respectively. The thin dielectric waveguide with high permittivity is here used as the metal wire of conventional wire antennas, due to its traveling-wave radiation under  $TM_{01}$  mode. The different radiation characteristics of the electrically small loop and full-wave loop antennas are discussed. And the dielectric large half-loop antenna with ground plane and bi-directional radiation is utilized to form a Yagi-Uda array for desired end-fire radiation. Moreover, circular loop elements are subsequently transformed into rectangular shape to reduce the profile of antenna and a comparison between the conventional metal Yagi-Uda antenna and the proposed dielectric one is provided. It is found that the dielectric parasitic element could play a more flexible role. Both ceramic and pure-water antenna prototypes are fabricated and tested. Measured results match the simulated ones well, which validates the predicted antenna performance.

**INDEX TERMS** Dielectric Yagi-Uda antenna, end-fire radiation, half-loop antenna, high-permittivity material, pure water, zirconia ceramic.

## I. INTRODUCTION

WITH the requirement for long-distance terrestrial directional communication, end-fire antennas have drawn many research interests. Several kinds of classical antennas have been proposed to support end-fire radiation, such as Yagi-Uda antennas [1], [2], [3], [4], [5], log-periodic antennas [6], [7], [8], surface-wave antennas [9], [10], and some leaky-wave antennas with fixed beam [11], [12], [13]. However, the aforementioned end-fire antennas are usually made of metal materials, which would inevitably suffer from conductor loss and limited radiation efficiency especially at high frequency.

Dielectric antennas have intrinsic superiority in radiation efficiency and sizing flexibility. Until now, many efforts

have been made on the design of dielectric antennas with end-fire radiation [14], [15], [16], [17], [18], [19], [20], [21]. And these proposed design methods can be generally divided into two categories. The first one is to utilize the surface-wave radiation of dielectric structure [14], [15], [16], [17]. By virtue of gradual changing shape or permittivity of dielectric, end-fire beam can be realized. However, this kind of dielectric end-fire antenna usually needs an extra surface wave launcher, which increases the complexity of antenna structure. In [17], four dielectric sections with tapered permittivities compose a wideband end-fire antenna, where the first section acts as a surface wave launcher to simplify the structure of excitation. But the used dielectric blocks with different infill ratios increase the difficulty of processing.

The second method for designing dielectric end-fire antenna is to form a complementary structure, which combines the equivalent magnetic dipole and electric dipole [18], [19], [20], [21]. By controlling the magnetoelectric resonances from the fundamental and higher-order modes of a dielectric resonator antenna (DRA), or a hybrid DRA with parasitic slot or probe, the desired lateral radiation could be achieved. But this kind of dielectric end-fire antenna usually normally has a high profile.

As a type of classical wire antenna, the conventional metal Yagi-Uda loop antenna with simple structure can support end-fire radiation [22], [23], [24]. And it is known that the loop antenna can be transformed into a half-loop one with ground plane to reduce its profile [25], [26]. According to the radiation mechanism of dielectric waveguide [27], [28], [29], a thin dielectric waveguide with high permittivity can be used just as the metal wire in conventional wire antennas, when it works at the cut-off state of  $TM_{01}$  mode. As such, a kind of half-loop Yagi-Uda antenna made of high-permittivity dielectric is proposed in this paper to realize desired end-fire radiation. Low-loss zirconia ceramic and liquid pure water are here adopted to implement the proposed antenna respectively, where the former contributes to attaining high radiation efficiency and the latter supports the characteristic of pattern reconfigurability by controlling its filling state. Compared with the reported dielectric Yagi antennas adopted dipole or monopole structure [30], [31], the proposed loop one has a driver element with bi-directional radiation rather than the omnidirectional one, meanwhile loop antenna possesses a lower profile.

## II. CONFIGURATION OF THE PROPOSED DIELECTRIC HALF-LOOP YAGI-UDA ANTENNA

Fig. 1 depicts the configuration of proposed dielectric half-loop Yagi-Uda antenna. It is seen that the proposed antenna consists of three dielectric rectangular half loops which play the roles of driver, reflector, and director respectively, a metal ground, as well as a coaxial probe connected with the driver loop. One of ends of the driver is suspended to avoid short circuit where a thin Teflon cylinder with a height of  $h_t$  is exactly inserted underneath the end. The probe passes through the Teflon cylinder and dips into the driver to excite the desired operating mode. The height above the ground of the probe is marked as  $h_p$ . The lengths and heights of three dielectric loops are denoted as  $l$ ,  $l_1$ ,  $l_2$ , and  $h$ ,  $h_1$ ,  $h_2$ , respectively. The radii of their cross sections are  $r_c$ ,  $r_{c1}$ , and  $r_{c2}$ . The metal ground is square with the size of  $L_g \times W_g$  and a thickness of  $t$ . The main dimensions of the proposed dielectric half-loop Yagi-Uda antenna are provided here as follows:  $L_g = 180$  mm,  $W_g = 180$  mm,  $r_c = 2.5$  mm,  $r_{c1} = 2.75$  mm,  $r_{c2} = 1.75$  mm,  $h = 11$  mm,  $h_1 = 11.5$  mm,  $h_2 = 12.5$  mm,  $l = 43$  mm,  $l_1 = 43.5$  mm,  $l_2 = 43.5$  mm,  $h_t = 1$  mm,  $h_p = 3$  mm,  $t = 2$  mm,  $d_1 = 15$  mm,  $d_2 = 8$  mm.

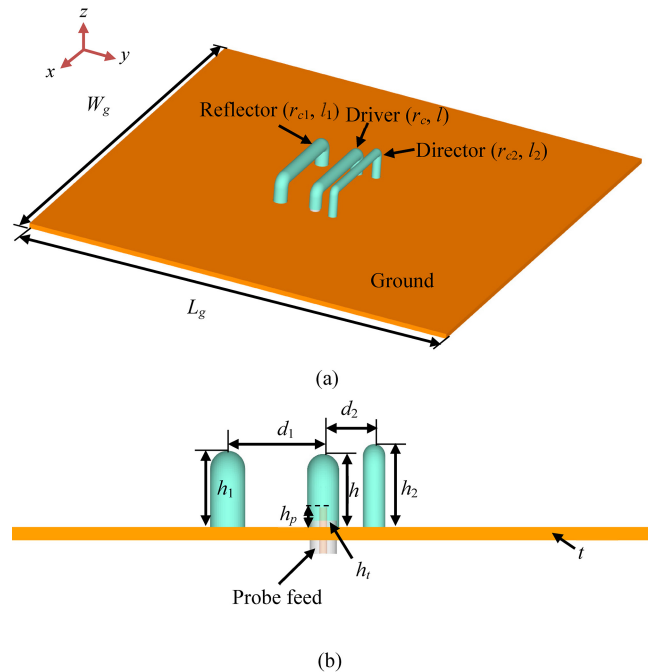


FIGURE 1. Configuration of the proposed dielectric half-loop Yagi-Uda antenna. (a) 3-D view. (b) Side view.

## III. WORKING PRINCIPLE OF THE PROPOSED DIELECTRIC HALF-LOOP ANTENNA

Firstly, the working principles of the dielectric half-loop antenna including the radiation mechanism of dielectric waveguide and radiation characteristics of dielectric half-loop antenna are discussed in this section.

### A. RADIATION MECHANISM OF DIELECTRIC WAVEGUIDE

According to our previous work [27], [28], [29], it is known that a dielectric waveguide can support leaky-wave radiation when it works at the cut-off state of high-order mode. And as one of high-order modes, the  $TM_{01}$  mode can be quite easily excited by a probe feed. Moreover, it is found that a dielectric waveguide operating at the cut-off state of  $TM_{01}$  mode has similar radiation characteristics to the metal long wire. In this context, the thin dielectric waveguide with high permittivity can be utilized as the metal wire of conventional wire antennas. The working frequency  $f$  within the cut-off region of  $TM_{01}$  mode satisfies:

$$0 < f < \frac{2.405c}{\pi d \sqrt{\epsilon_r - 1}} \quad (1)$$

where  $c$  represents the speed of light in free space,  $d$  is the waveguide diameter,  $\epsilon_r$  and 1 represent the relative permittivities of dielectric and air, respectively.

To verify the aforementioned analysis, an example, i.e., a straight dielectric waveguide made of high-permittivity zirconia ceramic ( $\epsilon_r = 32$ ,  $\tan \delta = 0.002$ ), is here provided and fed by coaxial probe, as shown in Fig. 2. Fig. 3

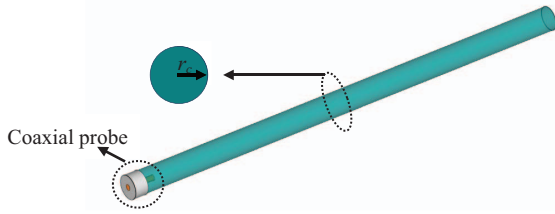


**FIGURE 2.** Configuration of a straight dielectric waveguide made of zirconia ceramic and fed by coaxial probe.

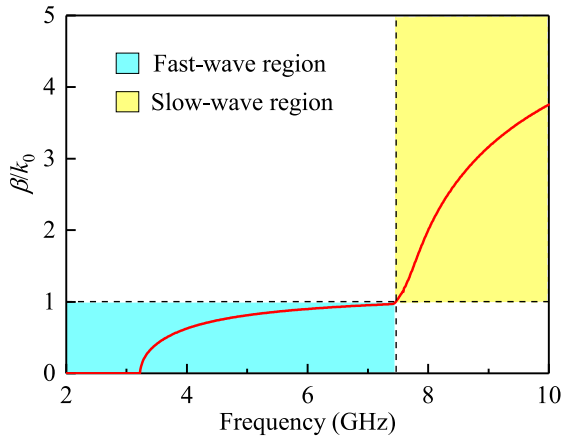


**FIGURE 3.** Extracted normalized phase constant ( $\beta/k_0$ ) for the dielectric waveguide operating at the  $TM_{01}$  mode.

exhibits the extracted normalized phase constant ( $\beta/k_0$ ) for the dielectric waveguide operating at the  $TM_{01}$  mode. It is clear that the dielectric waveguide works as a fast-wave system when the operating frequency is lower than the cut-off one. Electric-field distributions at 5 GHz (cut-off region) along the dielectric waveguide and its cross-section plane are displayed in Fig. 4, which further demonstrate the radiation mechanism of dielectric waveguide. It is seen that the electric-field distribution at cross-section plane is radially symmetric, which reveals the  $TM_{01}$  mode. Besides, a clear process about the power leakage of dielectric waveguide is observed owing to the fast-wave system.

### B. RADIATION CHARACTERISTICS OF DIELECTRIC HALF-LOOP ANTENNA

As one of primary antenna shapes, the loop antenna possesses a simple structure, but it could support various radiation characteristics based on different dimensions. Fig. 5 shows the configurations of conventional metal small and large loop antennas, as well as their radiation patterns at the plane perpendicular to loop. It is obvious that for the electrically small loop and full-wave loop, the phase distributions of their surface currents along loop are different, which leads to different radiation patterns. For the small loop, the phase discrepancy can be omitted, and the radiation mostly concentrates on the direction along the loop. But for the large loop, the beam usually points to the broadside because of the phase distribution.

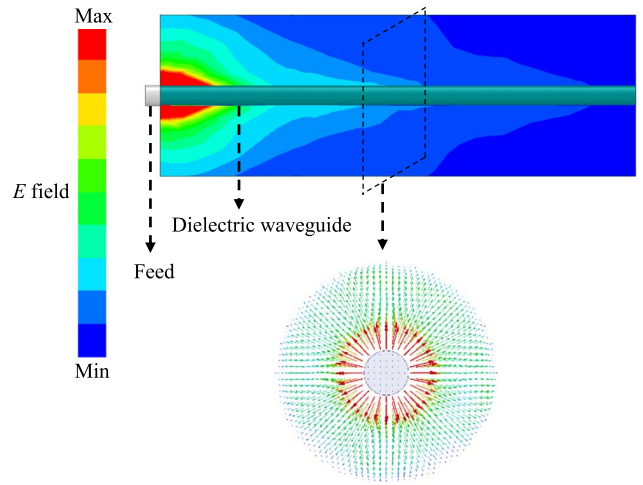


**FIGURE 4.** Electric-field distributions at 5 GHz (cut-off region) along the dielectric waveguide and its cross-section plane.

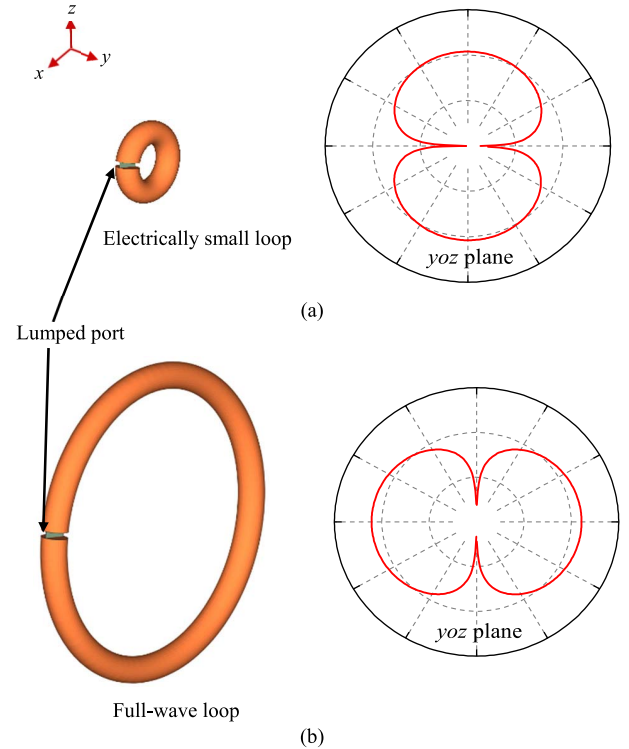


**FIGURE 5.** Configurations of conventional metal small and large loop antennas, as well as their radiation patterns at the plane perpendicular to loop. (a) Electrically small loop. (b) Full-wave loop.

By replacing the conventional metal wire with the thin high-permittivity dielectric waveguide and introducing the ground plane to adapt practical applications, a kind of dielectric half-loop antenna made of zirconia ceramic is then proposed, as shown in Fig. 6. Compared with full-loop antenna, the half-loop one has a lower profile and a much simpler feed structure where a pair of differential inputs can be simplified as a single probe.

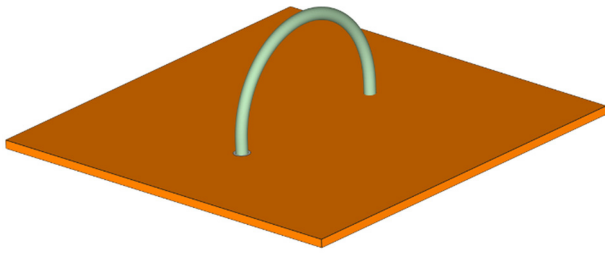


**FIGURE 6.** Configuration of the proposed dielectric half-loop antenna made of zirconia ceramic.

The radiation characteristics of dielectric small and large half-loop antennas are also investigated, as provided in Fig. 7. It is seen that after adopting the ground, the dielectric small and large half-loop antennas support broadside and bi-directional radiation, respectively. And it is clear that the large one is suitable to serve as a driver in a Yagi-Uda array.

#### IV. DIELECTRIC HALF-LOOP YAGI-UDA ANTENNA

By using the aforementioned dielectric half-loop structure as a driver, a dielectric half-loop Yagi-Uda antenna is proposed and discussed in this section.

##### A. OPERATION MECHANISM OF DIELECTRIC HALF-LOOP YAGI-UDA ANTENNA

Actually, the operation mechanism of dielectric half-loop Yagi-Uda antenna is similar to the conventional metal one. It is known that the radiation of a Yagi-Uda antenna is a superposition of the driver and the parasitic elements. For a two-element Yagi-Uda antenna, its array factor can be expressed as a function of the polar angle ( $\theta$ ) [32]:

$$AF = 1 + me^{j(\alpha + k_0 d \sin \theta)} \quad (2)$$

where  $m$  is the amplitude ratio,  $\alpha$  is the phase offset of the parasitic element from the driver,  $k_0$  is the free-space wavenumber,  $d$  is the distance between two elements. It is clear that the parasitic element acting as a director or reflector depends on the value of  $d$  and  $\alpha$ , where  $\alpha$  is affected by  $d$  and the length of the parasitic element in the conventional metal Yagi-Uda antenna. And for the dielectric case, the radius (cross section) of the dielectric waveguide would also affect  $\alpha$ . Therefore, the distance from the parasitic element to the driver, as well as the length and the radius (cross section) of the dielectric parasitic element are the key factors in the design of the proposed dielectric Yagi-Uda antenna.

It should be mentioned that compared with the conventional metal half-loop Yagi-Uda antenna, the proposed dielectric one possesses an extra degree of freedom in its design process, i.e., the radius of cross section, which can be utilized to attain a better performance.

##### B. TWO-ELEMENT DIELECTRIC HALF-LOOP YAGI-UDA ANTENNA

A two-element dielectric half-loop Yagi-Uda antenna is designed to investigate the influence of the parasitic loop, as

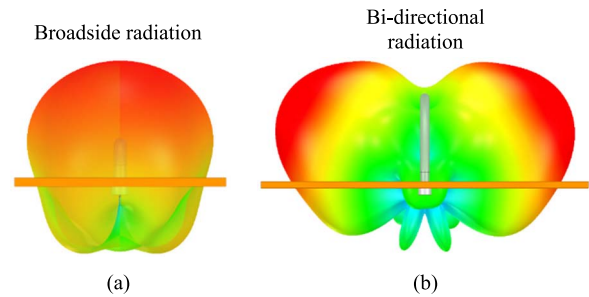


**FIGURE 7.** Radiation of the dielectric small and large half-loop antennas. (a) Small half-loop antenna. (b) Large half-loop antenna.

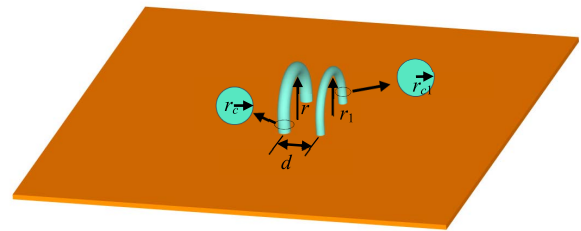


**FIGURE 8.** Configuration of the dielectric two-element half-loop Yagi-Uda antenna. ( $r = 15$  mm,  $r_c = 2.5$  mm)

shown in Fig. 8. Considering that the ground would result in tilted beam with unfixed angle, the front-to-back ratio (FBR) is modified to correct the impact where the main and back lobes are flexibly determined at tilted angle rather than the fixed direction. Fig. 9 depicts the modified FBR of the dielectric two-element half-loop Yagi-Uda antenna under different values of  $r_1$ ,  $d$ , and  $r_{c1}$ . It is found that the dielectric Yagi-Uda antenna is similar to the metal one. The role of parasitic loop is also determined by its dimensions and the space from the driver. For example, assuming the values of  $d$  and  $r_{c1}$  are 5 mm and 2 mm respectively, the parasitic loop can serve as a director when the loop radius  $r_{c1}$  is less than 18 mm, and then it turns into a reflector with the increase of  $r_{c1}$ . It is seen that big  $r_1$ ,  $d$ , and  $r_{c1}$  are helpful to attain a reflector, which is also corresponding to the experiences in the design of a metal Yagi-Uda antenna.

##### C. THREE-ELEMENT DIELECTRIC HALF-LOOP YAGI-UDA ANTENNA

In order to realize better directionality, a three-element dielectric half-loop Yagi-Uda antenna is then proposed. Fig. 10 shows its configuration and radiation patterns of E-plane and H-plane at 5.4 GHz. It is seen that the proposed three-element Yagi-Uda antenna has end-fire beam with angle of 60 degrees and its radiation gain exceeds 10 dBi. However, the half-loop structure with circular shape leads to a high profile of the proposed antenna.

##### D. DIELECTRIC RECTANGULAR HALF-LOOP YAGI-UDA ANTENNA

Circular loop elements are subsequently transformed into rectangular shape to reduce the profile of antenna, as shown

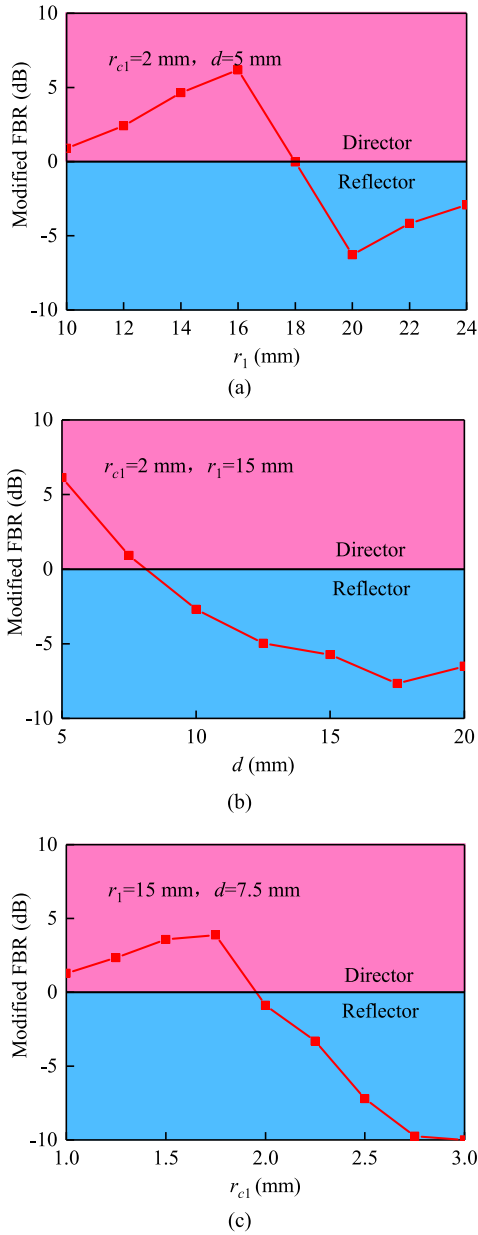


FIGURE 9. Modified front-to-back ratio (FBR) of the dielectric two-element half-loop Yagi-Uda antenna under different values of (a)  $r_1$ . (b)  $d$ . (c)  $r_{cl}$ .

in Fig. 11. It is clear that the profile of the rectangular half-loop Yagi-Uda antenna is much lower than the circular loop one. As to the radiation performance, its radiation patterns at 5.4 GHz are also provided, which are similar to those of the circular half-loop Yagi-Uda antenna. Fig. 12 shows the electric-field distributions at  $yo$ z plane of the dielectric rectangular half-loop Yagi-Uda antenna operating at 5.4 GHz. It is seen that the strong coupling is generated among the driver, director and reflector. And the electromagnetic waves are mainly concentrated on the director side, leading to the end-fire radiation and high FBR.

In order to reveal the design flexibility of the proposed dielectric Yagi-Uda antenna, Fig. 13 shows the discrepancy between the effects on the modified FBR of dielectric and

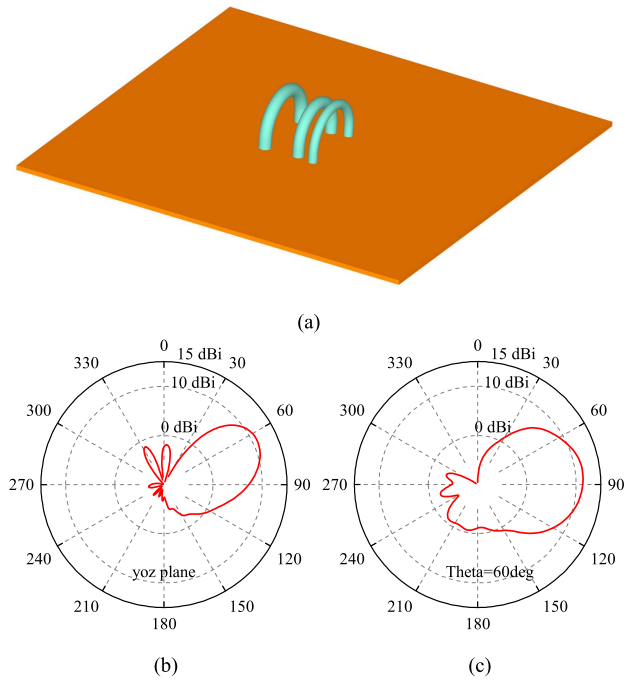


FIGURE 10. Configuration of a dielectric three-element half-loop Yagi-Uda antenna and its radiation patterns at 5.4 GHz. (a) 3-D view. (b) E-plane. (c) H-plane.

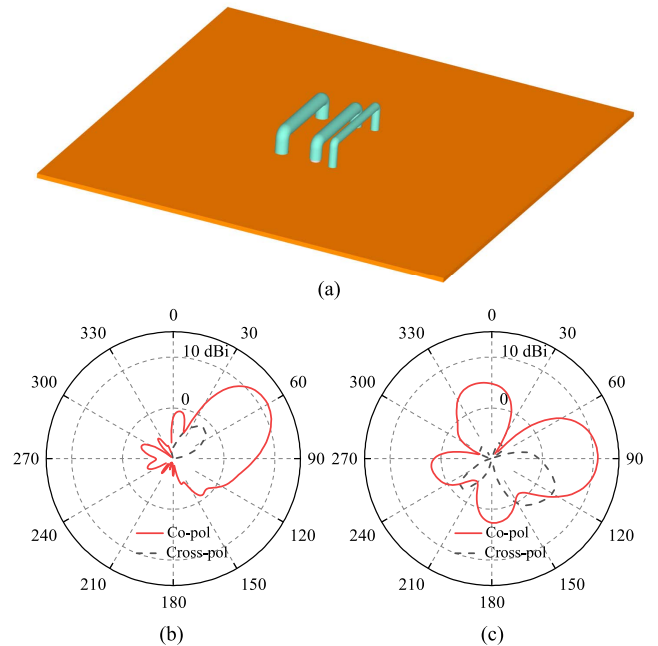


FIGURE 11. Configuration of the dielectric rectangular half-loop Yagi-Uda antenna and its radiation patterns at 5.4 GHz. (a) 3-D view. (b) E-plane. (c) H-plane.

metal parasitic elements. It is worth mentioning that a typical case where the parasitic element mainly plays the role of reflector is here adopted since the operating principle is same no matter in reflector or director case. Therefore, both the dielectric and metal parasitic loops are longer than the driver. According to Fig. 13, it is clear that when the distance

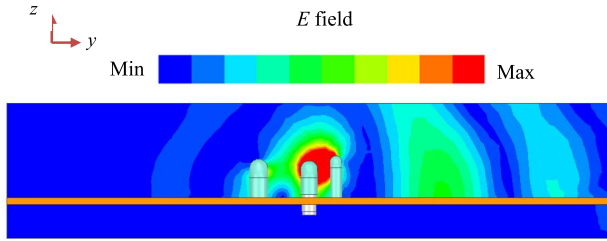


FIGURE 12. Electric-field distributions at 5.4 GHz of the dielectric rectangular half-loop Yagi-Uda antenna.

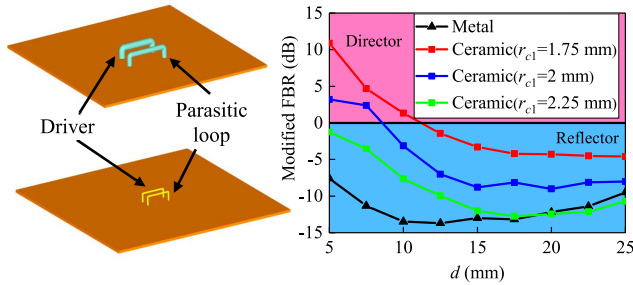


FIGURE 13. The discrepancy between the effects on the modified front-to-back ratio (FBR) of dielectric and metal parasitic elements.

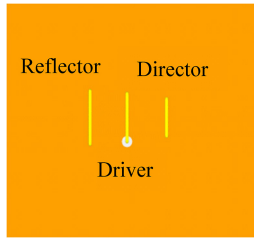


FIGURE 14. Configuration of a conventional three-element metal half-loop Yagi-Uda antenna.

between the driver and reflector ranges from  $0.1 \sim 0.4 \lambda$  ( $\lambda$ : wavelength), it is found that the metal parasitic loop always acts as a reflector, which is corresponding to the classical theory. As to the dielectric one, its cross section affecting the working frequency provides an extra degree of freedom, which is different from the metal one. The role of the dielectric parasitic loop is determined by the dimension of its cross section and the space from the driver. Therefore, although the parasitic loop is longer than the driver, it can still play the role of director under different radii. Due to the different radiation principles of dielectric waveguide and metal wire, the design of dielectric half-loop Yagi-Uda antenna is more flexible, which is helpful for the compact structure. For the metal half-loop Yagi-Uda antenna, the reflector and driver are often close to each other, while the director is a little far from the driver so as to obtain good directivity, as shown in Fig. 14. The spaces from the reflector and director to the driver are usually about  $0.25 \lambda$ . But as to the dielectric one, according to Fig. 13, a good dielectric director near the driver could be achieved, which exactly contributes to the compact structure of proposed three-element Yagi-Uda antenna shown in Fig. 1.

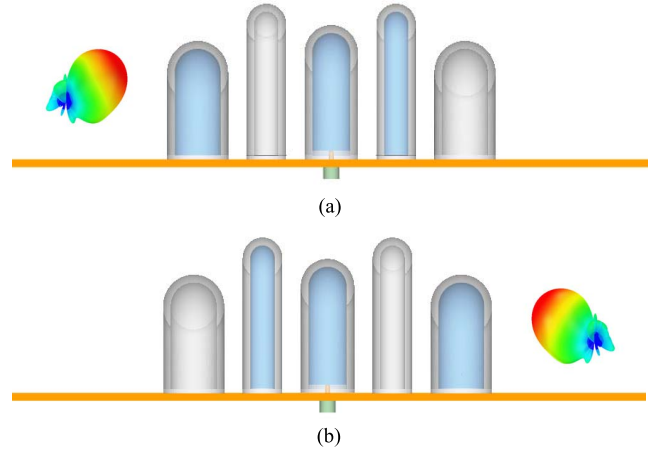


FIGURE 15. Dynamic cases for pattern reconfigurability of a pure-water half-loop Yagi-Uda antenna. (a) Case 1. (b) Case 2.

TABLE 1. Performance comparison between the conventional metal and proposed dielectric half-loop Yagi-Uda antennas.

Performance	Antenna	Dielectric one	Metal one
Impedance bandwidth		4.6 - 5.64 GHz	5.08 - 5.42 GHz
3-dB gain bandwidth		4.42 - 5.73 GHz	4.92 - 5.78 GHz
Maximal radiation gain		11.4 dBi	11.1 dBi
Distance from driver to director		8 mm	16 mm
Modified FBR (5.4 GHz)		14.7 dB	15.1 dB

Table 1 provides a comparison between the conventional metal and proposed dielectric half-loop Yagi-Uda antennas. It is clear that both antennas have similar radiation gains and FBRs, while the dielectric one possesses the smaller distance from the driver to the director, and it also has wider operating band owing to its traveling-wave structure.

It is known to all that pure water has high permittivity and fluidity. Therefore, the dielectric rectangular half-loop Yagi-Uda structure can be implemented by pure water to achieve reconfigurability. Fig. 15 sketches the dynamic cases for pattern reconfigurability of a pure-water half-loop Yagi-Uda antenna. Five containers prepared for water are bilaterally symmetrical. By controlling the filling state of water in different containers, the director and reflector can be mirrored at symmetrical locations, which leads to the pattern reconfigurability.

## V. FABRICATION AND EXPERIMENTAL RESULTS

Both the ceramic half-loop Yagi-Uda antenna made of zirconia and pattern-reconfigurable pure-water half-loop Yagi-Uda antenna are fabricated and tested.

### A. CERAMIC HALF-LOOP YAGI-UDA ANTENNA

By virtue of the ceramic 3-D printing technology based on vat photopolymerization (VPP) [33], the driver, reflector, and director made of zirconia ceramic can be fabricated with high precision and purity. Fig. 16 shows the fabricated ceramic half-loop Yagi-Uda antenna prototype. A coaxial probe is

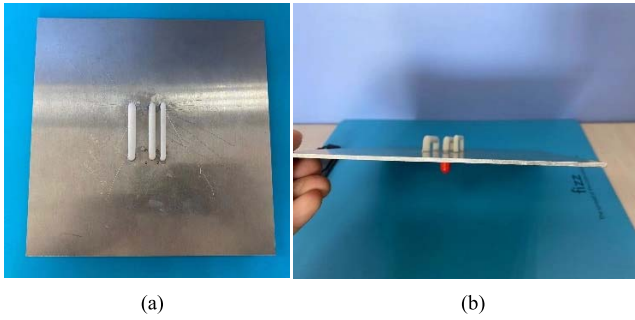


**FIGURE 16.** Photographs of the fabricated ceramic half-loop Yagi-Uda antenna prototype. (a) Top view. (b) Side view.

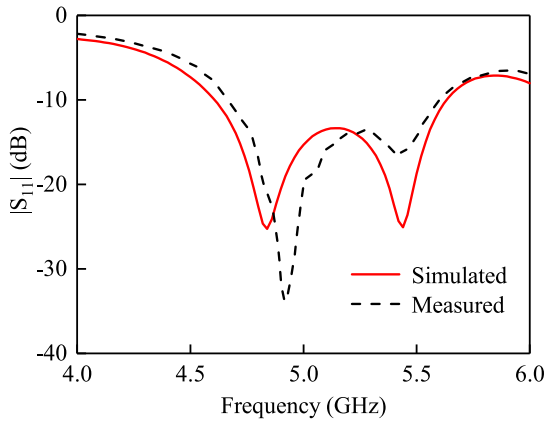


**FIGURE 17.** Simulated and measured reflection coefficients of the fabricated ceramic half-loop Yagi-Uda antenna prototype.

well installed by the reserved holes on the ground and driver. The 3-D printing and postprocessing are guided by 3dpro Technology Co., Ltd.

Fig. 17 depicts the simulated and measured reflection coefficients of the fabricated ceramic half-loop Yagi-Uda antenna prototype. It is found that the measured result shows a great agreement with the simulated one and it covers a wide frequency range from 4.67 to 5.6 GHz, which is little narrower than the simulated result.

Simulated and measured radiation gains of the fabricated ceramic half-loop Yagi-Uda antenna prototype are provided in Fig. 18. It is observed that a good agreement between the measured and simulated results is obtained. The fabricated ceramic antenna prototype possesses stable radiation gain with the maximum value of 11.04 dBi and its 3-dB gain bandwidth covers from 4.3 to 5.65 GHz. The simulated power tolerance of proposed ceramic half-loop Yagi-Uda antenna is about 792 kW.

Fig. 19 shows the simulated and measured normalized radiation patterns of the fabricated ceramic half-loop Yagi-Uda antenna prototype operating at 5.4 GHz. It is seen that the fabricated antenna supports the end-fire radiation with the beam angle of 60 degrees. Besides, the main beam of the measured E-plane is slightly split, and that of the measured H-plane is little wider than the simulated result.

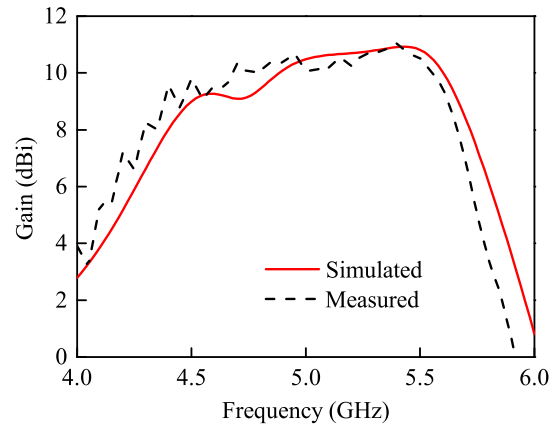


**FIGURE 18.** Simulated and measured radiation gains of the fabricated ceramic half-loop Yagi-Uda antenna prototype.

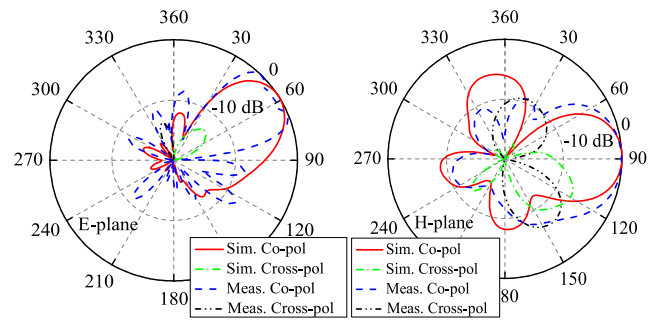


**FIGURE 19.** Simulated and measured normalized radiation patterns of the fabricated ceramic half-loop Yagi-Uda antenna prototype operating at 5.4 GHz.

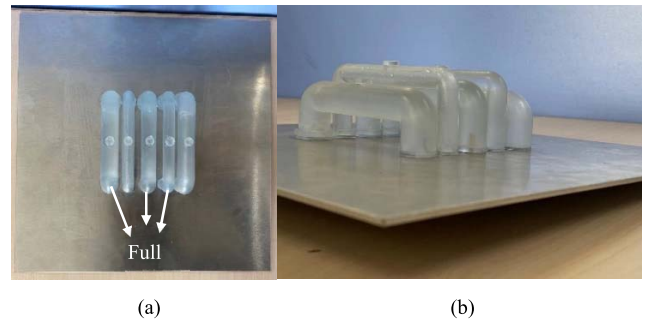


**FIGURE 20.** Photographs of the fabricated pattern-reconfigurable pure-water half-loop Yagi-Uda antenna prototype (Case 1). (a) Top view. (b) Side view.

## B. PATTERN-RECONFIGURABLE WATER HALF-LOOP YAGI-UDA ANTENNA

By using stereolithography apparatus (SLA) craft, one of 3-D printing technologies, transparent containers prepared for pure water can be easily fabricated. Fig. 20 exhibits the fabricated pattern-reconfigurable pure-water half-loop Yagi-Uda antenna prototype. It is seen that some plugs are here utilized for the convenience of moving water. For the arbitrary working case of the fabricated water antenna, three half-loop containers are full of distilled water ( $\epsilon_r = 78.4$ ,  $\tan \delta = 0.08$  @ 1.8 GHz) and the rest of containers keep empty.

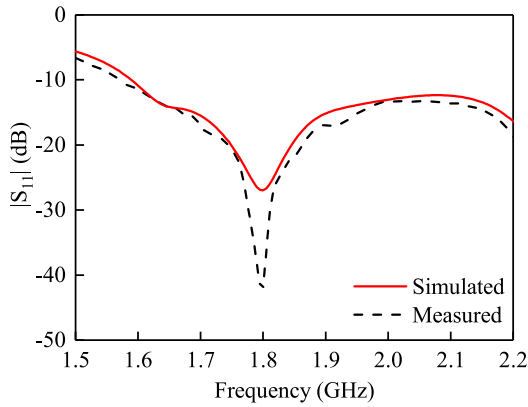


**FIGURE 21.** Simulated and measured reflection coefficients of the fabricated pattern-reconfigurable pure-water half-loop Yagi-Uda antenna prototype (Case 1).

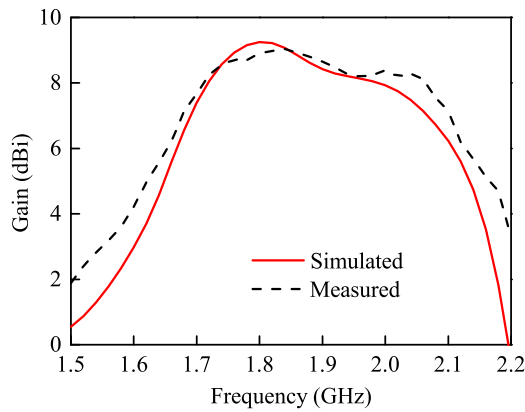


**FIGURE 22.** Simulated and measured radiation gains of the fabricated pattern-reconfigurable pure-water half-loop Yagi-Uda antenna prototype (Case 1).

In consideration of that pure water suffers from huge dielectric loss at high frequency, the water antenna is designed at an acceptable spectrum to ensure the radiation efficiency above 70%. In addition, since the two cases of pattern reconfigurability are fully mirrored with each other and the results of two cases are almost same, only the measured results under Case 1 are provided. Fig. 21 provides the simulated and measured reflection coefficients of the fabricated pattern-reconfigurable pure-water half-loop Yagi-Uda antenna prototype. It is clear that the measured and simulated results are in good agreement. And the fabricated antenna has a wide impedance bandwidth covering from 1.59 to 2.2 GHz.

Fig. 22 depicts the simulated and measured radiation gains of the fabricated pattern-reconfigurable pure-water half-loop Yagi-Uda antenna prototype. It is observed that the measured gain matches the simulated one well. The fabricated antenna has a maximal gain of 9.04 dBi and its 3-dB gain bandwidth ranges from 1.66 to 2.12 GHz. The simulated power tolerance of proposed pattern-reconfigurable pure-water half-loop Yagi-Uda antenna is about 223 kW.

The simulated and measured normalized radiation patterns of the fabricated pattern-reconfigurable pure-water half-loop Yagi-Uda antenna prototype operating at 1.8 GHz are

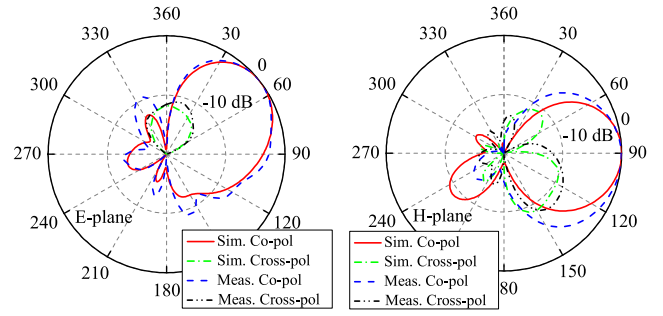


**FIGURE 23.** Simulated and measured normalized radiation patterns of the fabricated pattern-reconfigurable pure-water half-loop Yagi-Uda antenna prototype operating at 1.8 GHz (Case 1).

**TABLE 2.** Comparison among pattern-reconfigurable Yagi-Uda antennas.

Ref.	Tuning mechanism	Maximum gain (dBi)	Radiation efficiency	Impedance bandwidth	FBR	Reaction time
[34]	PIN diodes	5.27	53.3%	548-580 MHz	10 dB	ms or $\mu$ s level
[35]	PIN diodes	7.3	70%-85%	3.32-3.51 GHz	12 dB	ms or $\mu$ s level
[36]	PIN diodes	6.2	81.6%-93%	2.3-2.5 GHz	15 dB	ms or $\mu$ s level
This work	Pure water	9.21	70%-86%	1.59-2.2 GHz	12.7 dB	10-100 s

exhibited in Fig. 23. It is found that the measured and simulated results of E-plane including both co-polarization and cross-polarization are in good agreement, while the measured main beam of H-plane is little wider than that of the simulated one.

Table 2 tabulates a comparison among Yagi-Uda antennas with pattern reconfigurability. It is seen that compared with those designs tuned by PIN diodes [34], [35], [36], the proposed pure-water one has similar FBR and radiation efficiency, but possessing higher radiation gain and wider impedance bandwidth. Besides, the water antenna needs longer reaction time for reconfiguring and it is more beneficial for those systems with no need to require fast tuning process.

## VI. CONCLUSION

In this paper, a kind of dielectric half-loop Yagi-Uda antenna with end-fire radiation is proposed by adopting high-permittivity material. Two antenna prototypes made of zirconia ceramic and pure water respectively, are here implemented to demonstrate the proposed concept. The traveling-wave radiation from dielectric waveguide and 3-D printing technology are utilized respectively in the operation and fabrication of the proposed antenna. The proposed dielectric half-loop Yagi-Uda antenna can take full advantage of dielectric material, such as high radiation efficiency by low-loss dielectric and reconfigurability by liquid dielectric. Besides, benefiting from the extra degree of freedom, i.e., the cross-section radius of dielectric waveguide, the design



of proposed dielectric half-loop Yagi-Uda antenna is more flexible, which is ease to achieve compact structure. This work provides a simple method for the design of an end-fire dielectric antenna without an extra surface wave launcher.

## REFERENCES

- [1] Z. Hu, Z. Shen, W. Wu, and J. Lu, "Low-profile top-hat monopole Yagi antenna for end-fire radiation," *IEEE Trans. Antennas Propag.*, vol. 63, no. 7, pp. 2851–2857, Jul. 2015.
- [2] J. Liu and Q. Xue, "Microstrip magnetic dipole Yagi array antenna with endfire radiation and vertical polarization," *IEEE Trans. Antennas Propag.*, vol. 61, no. 3, pp. 1140–1147, Mar. 2013.
- [3] Y. Luo and Q.-X. Chu, "A Yagi-Uda antenna with a stepped-width reflector shorter than the driven element," *IEEE Antennas Wireless Propag. Lett.*, vol. 15, pp. 564–567, 2016.
- [4] S. Wang et al., "A planar absorptive-branch-loaded quasi-Yagi antenna with filtering capability and flat gain," *IEEE Antennas Wireless Propag. Lett.*, vol. 20, no. 9, pp. 1626–1630, Sep. 2021.
- [5] H. Zhou, J. Geng, and R. Jin, "A magnetic Yagi-Uda antenna with vertically polarized endfire radiation in millimeter-wave band applying higher order mode," *IEEE Trans. Antennas Propag.*, vol. 70, no. 10, pp. 8941–8950, Oct. 2022.
- [6] Z. Hu, Z. Shen, W. Wu, and J. Lu, "Low-profile log-periodic monopole array," *IEEE Trans. Antennas Propag.*, vol. 63, no. 12, pp. 5484–5491, Dec. 2015.
- [7] Q. Chen, Z. Hu, Z. Shen, and W. Wu, "2–18 GHz conformal low-profile log-periodic array on a cylindrical conductor," *IEEE Trans. Antennas Propag.*, vol. 66, no. 2, pp. 729–736, Feb. 2018.
- [8] J. Pu and B. Zhang, "Redundancy elimination of the classic log-periodic dipole array antenna by resonance point optimization for a miniaturized structure," *IEEE Trans. Antennas Propag.*, vol. 69, no. 12, pp. 8345–8353, Dec. 2021.
- [9] Y. Hou, Y. Li, Z. Zhang, and M. F. Iskander, "Microstrip-fed surface-wave antenna for endfire radiation," *IEEE Trans. Antennas Propag.*, vol. 67, no. 1, pp. 580–584, Jan. 2019.
- [10] J. Liang and J. Liu, "A low-profile planar surface-wave antenna with metasurface for endfire radiation," *IEEE Antennas Wireless Propag. Lett.*, vol. 19, no. 12, pp. 2452–2456, Dec. 2020.
- [11] P. Liu, Y. Li, Z. Zhang, and P. Jia, "All-metal centipede-like end-fire antenna," *IEEE Antennas Wireless Propag. Lett.*, vol. 17, no. 10, pp. 1905–1909, Oct. 2018.
- [12] L. Sun, Y. Hou, Y. Li, Z. Zhang, and Z. Feng, "An open cavity leaky-wave antenna with vertical-polarization endfire radiation," *IEEE Trans. Antennas Propag.*, vol. 67, no. 5, pp. 3455–3460, May 2019.
- [13] Z. Wu, Z. Miao, R. Gao, and L. Xiao, "Series-fed all-metal and wide-axial-ratio-bandwidth circularly polarized leaky-wave antenna with endfire radiation," *IEEE Antennas Wireless Propag. Lett.*, vol. 21, no. 4, pp. 646–650, Apr. 2022.
- [14] Z. Chen and Z. Shen, "Wideband flush-mounted surface wave antenna of very low profile," *IEEE Trans. Antennas Propag.*, vol. 63, no. 6, pp. 2430–2438, Jun. 2015.
- [15] P. Wang and Z. Shen, "End-fire surface wave antenna with metasurface coating," *IEEE Access*, vol. 6, pp. 23778–23785, 2018.
- [16] Y. Cai, Z. Qian, Y. Zhang, and W. Cao, "A compact wideband SIW-fed dielectric antenna with end-fire radiation pattern," *IEEE Trans. Antennas Propag.*, vol. 64, no. 4, pp. 1502–1507, Apr. 2016.
- [17] J. Huang, S. J. Chen, Z. Xue, W. Withayachumnankul, and C. Fumeaux, "Wideband endfire 3-D-printed dielectric antenna with designable permittivity," *IEEE Antennas Wireless Propag. Lett.*, vol. 17, no. 11, pp. 2085–2089, Nov. 2018.
- [18] L. Guo, K. W. Leung, and Y. M. Pan, "Compact unidirectional ring dielectric resonator antennas with lateral radiation," *IEEE Trans. Antennas Propag.*, vol. 63, no. 12, pp. 5334–5342, Dec. 2015.
- [19] Y. M. Pan, K. W. Leung, and L. Guo, "Compact laterally radiating dielectric resonator antenna with small ground plane," *IEEE Trans. Antennas Propag.*, vol. 65, no. 8, pp. 4305–4310, Aug. 2017.
- [20] L. Guo, K. W. Leung, and N. Yang, "Wide-beamwidth unilateral dielectric resonator antenna using higher-order mode," *IEEE Antennas Wireless Propag. Lett.*, vol. 18, no. 1, pp. 93–97, Jan. 2019.
- [21] M. Boyuan, J. Pan, S. Huang, D. Yang, and Y.-X. Guo, "Wideband endfire dielectric resonator antenna employing fundamental and higher order magnetoelectric resonances," *IEEE Antennas Wireless Propag. Lett.*, vol. 20, no. 12, pp. 2524–2528, Dec. 2021.
- [22] J. Appel-Hansen, "The loop antenna with director arrays of loops and rods," *IEEE Trans. Antennas Propag.*, vol. 20, no. 4, pp. 516–517, Jul. 1972.
- [23] T. Korekado, K. Okuno, and S. Kurazono, "Design method of Yagi-Uda two-stacked circular loop array antennas," *IEEE Trans. Antennas Propag.*, vol. 39, no. 8, pp. 1112–1118, Aug. 1991.
- [24] Q. Lou, R.-X. Wu, and Y. Tian, "A rectangular loop Yagi-Uda antenna by the two materials 3-D printing technology," *IEEE Antennas Wireless Propag. Lett.*, vol. 17, no. 11, pp. 2017–2020, Nov. 2018.
- [25] G. Zhou and G. S. Smith, "An accurate theoretical model for the thin-wire circular half-loop antenna," *IEEE Trans. Antennas Propag.*, vol. 39, no. 8, pp. 1167–1177, Aug. 1991.
- [26] S. Krishnan, L.-W. Li, and M.-S. Leong, "A V-shaped structure for improving the directional properties of the loop antenna," *IEEE Trans. Antennas Propag.*, vol. 53, no. 6, pp. 2114–2117, Jun. 2005.
- [27] S. Wang et al., "Radar cross-section reduction of helical antenna by replacing metal with 3-D printed zirconia ceramic," *IEEE Antennas Wireless Propag. Lett.*, vol. 19, no. 2, pp. 350–354, Feb. 2020.
- [28] F. Fan et al., "Sub-6 GHz ceramic inverted-L antenna with non-resonant structure and leaky-wave radiation," *Appl. Phys. Lett.*, vol. 119, Jul. 2021, Art. no. 33501.
- [29] C. Hua et al., "Reconfigurable antennas based on pure water," *IEEE Open J. Antennas Propag.*, vol. 2, pp. 623–633, 2021.
- [30] J. Hesselbarth, D. Geier, and M. A. B. Diez, "A Yagi-Uda antenna made of high-permittivity ceramic material," in *Proc. Loughborough Antennas & Propag. Conf. (LAPC)*, 2013, pp. 94–98.
- [31] Z. Hu, W. Wu, Z. Shen, and C. Hua, "A Yagi monopole antenna made of pure water," in *Proc. IEEE Int. Symp. Antennas Propag. USNC/URSI Nat. Radio Sci. Meeting*, 2015, pp. 2241–2242.
- [32] C. A. Balanis, *Antenna Theory: Analysis and Design*. New York, NY, USA: Wiley, 1997.
- [33] F. Zhang et al., "The recent development of vat photopolymerization: A review," *Addit. Manuf.*, vol. 48, Dec. 2021, Art. no. 102423.
- [34] C. Kittiyapunya and M. Krarikhsh, "A four-beam pattern reconfigurable Yagi-Uda antenna," *IEEE Trans. Antennas Propag.*, vol. 61, no. 12, pp. 6210–6214, Dec. 2013.
- [35] W.-Q. Deng, X.-S. Yang, C.-S. Shen, J. Zhao, and B.-Z. Wang, "A dual-polarized pattern reconfigurable Yagi patch antenna for microbase stations," *IEEE Trans. Antennas Propag.*, vol. 65, no. 10, pp. 5095–5102, Oct. 2017.
- [36] J. Lu, H. C. Zhang, P. H. He, M. Wang, and T. J. Cui, "Pattern reconfigurable Yagi antenna based on active corrugated stripline," *IEEE Trans. Antennas Propag.*, vol. 71, no. 1, pp. 1011–1016, Jan. 2023.



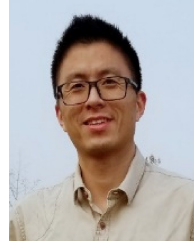
**WEN ZHENG** was born in Nanjing, Jiangsu, China, in 1997. He is currently pursuing the M.S. degree in electrical and automation engineering with Nanjing Normal University, Nanjing. His research interests include reflectionless antenna, dielectric antenna, and liquid antenna.



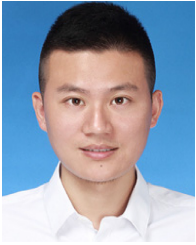
**SHIYANG WANG** (Member, IEEE) received the B.Eng. and Ph.D. degrees from the Nanjing University of Science and Technology, Nanjing, China, in 2014 and 2019, respectively. From 2017 to 2018, he joined as a Research Assistant with the University of Macau, Macau, China. He is currently with the School of Electrical and Automation Engineering, Nanjing Normal University. His research interests include microstrip patch antenna, liquid antenna, dielectric antenna, and 3-D printing technology.



**MENGJIAO TANG** was born in Xuzhou, Jiangsu, China, in 2002. She is majoring in automation with Nanjing Normal University, Nanjing. Her interests include dielectric antenna and 3-D printing technology.



**WANG REN** received the Ph.D. degree in electrical engineering from Zhejiang University, Hangzhou, China, in 2008. He joined Zhejiang Gongshang University in 2008, where he is currently working as an Assistant Professor. His research interests include multiband antenna design, ultrawide-band antenna design, and microwave power transfer.



**GANG ZHANG** (Senior Member, IEEE) received the Ph.D. degree in electronics and information engineering from Nanjing University of Science and Technology, Nanjing, China, in 2017.

He is currently working with School of Electrical and Automation Engineering, Nanjing Normal University, China. His research interest is miniaturized high performance microwave multifunctional passive component design and numerical synthesis methods in electromagnetics.

He has been an Associate Editor of *IET Electronics*

*Letters* and a Lead Guest Editor of *Frontiers in Physics* since 2020.



**CHANGZHOU HUA** (Member, IEEE) was born in Zhejiang, China, in 1984. He received the B.S. degree in electronics information engineering and the Ph.D. degree in communication engineering from the Nanjing University of Science and Technology, Nanjing, China, in 2007 and 2013, respectively.

He was a Visiting Researcher with the Department of Information and Electronic Engineering, Zhejiang University, Hangzhou, China, from 2009 to 2012. He was with the School of Electrical and Electronic Engineering, Nanyang Technological University, Singapore, as a Research Fellow from 2013 to 2015. He has been an Associate Professor with the Faculty of Electrical Engineering and Computer Science, Ningbo University, Ningbo, China, since April 2015. He has authored or coauthored more than 50 journal articles and conference papers. His research interests include microwave/millimeter-wave active and passive devices and circuits, lens antennas, and liquid antennas.